Fractals, Vol. 9, No. 4 (2001) 429–437

FRACTAL-SKELETAL BASED CHANNEL NETWORK (*F-SCN*) IN A TRIANGULAR INITIATOR-BASIN

B. S. DAYA SAGAR*, D. SRINIVAS† and B. S. PRAKASA RAO†
*Centre for Remote Imaging Sensing Processing (CRISP),
Faculty of Science, The National University of Singapore,
Lower Kent Ridge Road, Singapore 119260
†Centre for Remote Sensing and Information Systems,
Department of Geoengineering, Andhra University,
Visakhapatnam-530 003, India
*bsdsagar@hotmail.com
*bsdaya.sagar@mmu.edu.my

Received October 16, 2000; Accepted May 7, 2001

Abstract

Fractal-skeletal based channel network (*F-SCN*) model, which describes how the boundary of the basin constrains the channel network evolution, produces a channel network pattern that obeys Horton's laws. The statistical features of this model conform well with real networks. For this *F-SCN* that depends on general shape of the initiator-basin, generating mechanism and rule, and the nature of skeletonization process, the estimation of fractal dimension (D) is $\mathrm{Log}\, R_B/\mathrm{Log}\, R_L$. The estimated D, 1.76 is approximated to the observed value, 1.8.

1. INTRODUCTION

The corrugations in the basin outline can be visualized as topographic undulations. These undulations can be treated as the crenulations that are the flow paths of streams. It implies that the number of crenulations in the top most contour in the catchment is equal to the number of first order stream segments. After flowing to certain distance, two first order streams join to form a second order stream, the flow path of which is another crenulation, wider than that of the previous lower order crenulation. There will be less number of higher

*Current address: Faculty of Engineering and Technology (FET), Melaka Campus, Multimedia University, Jalan Ayer Keroh Lama, 75450, Melaka, Malaysia.

order channels than the lowest or lower orders, and also the crenulations. The two tributary branches arising at a stream segment bifurcation often differ in width, length and angle, leading to a highly heterogeneous structure. Although the basin shape is nearly the same, with a change in resolution, the existing stream orders in the small scale map will change in the corresponding large scale map. Hence, the process of stream order designation will be disturbed with a change in scale. If there are Ω orders in a basin of small scale, obviously $\Omega + n$ (n being scale-dependent) orders will be identified in the corresponding basin of larger scale.

One of the prevalent patterns of fractal trees is channel networks.[1] In the pattern of channel network, a channel continues to branch over many generations, and each of the smaller scale stream segments when magnified resemble the channel network as a whole. This property is termed "self-similarity." The stream network between trunk stream and twigs exhibits this property. The complex structure of the channel network sets the query why tributaries extend and bifurcate the way they do. The geometric pattern of such a stream network can be viewed as a "fractal" with a fractional dimension,[1] which can be employed as the basis of comparison of river basins. The quantitative expression of the drainage basin plays a consequential role in comprehending hydrological responses. To understand hydrological responses, several river network models that have originated from several concepts such as stochastic approach, invasion percolation theory, random theory, diffusion equations, cellular automata, diffusion limited aggregation (DLA) approach, an advective diffusion approach, and fractal-skeletal based theory have been developed in the last decade.[2–19]

Since the existing morphological skeleton within the fractal river basin is similar to the channel network pattern, this model is termed as a *fractal-skeletal based channel network* (*F-SCN*) model. However, this short note is an extension of the authors works. In the earlier work, a fractal relation of a morphological skeleton has been shown.[18] In the later works,[19] a deterministic approach has been followed to establish relationships among morphometric parameters of the *F-SCNs* where the regular sided initiator-basins ($4 < N < \infty$, N being a number of sides of the polygon) have been considered. However, the present paper deals with *F-SCNs* in a triangular initiator-basin to test whether the *F-SCN* follows Horton's laws, and to compute the fractal dimension by considering two morphometric quantities, namely bifurcation and length ratios. The organization of this short note is as follows. Section 2 deals with certain basic mathematical morphological transformations that are needed to extract channel network and the Horton's laws of stream number and length. In Sec. 3, *F-SCN* model is described, and a case study with results is furnished in Sec. 4.

2. MORPHOLOGY AND HORTON'S LAWS

2.1 Mathematical Morphology

Certain important transformations from the field of mathematical morphology such as *erosion*, *dilation* and *opening* transformations are presented. Mathematical morphology[20] based on set theoretic concepts is a remarkable approach in the analysis of geometric properties of different structures. The discrete binary image, M, is defined as a finite subset of Euclidean two-dimensional space, IR^2. The geometrical properties of M, which contained fractal basin (set) and non-fractal zone (set complement), were subjected to morphological functionals by means of a defined sub-image that is here by termed as a structuring element (S). Constraints that correspond to the four principles of the theory of mathematical morphology,[20] such as invariance under translation, compatibility with change of scale, local knowledge and the upper semi-continuity, are important in morphological transformations — erosion to contract, dilation to expand and cascade processes performed by means of structuring element. M and S are sets of Euclidean space with elements m and s, respectively; $m = (m_1, \ldots, m_n)$ and $s = (s_1, \ldots, s_n)$ being n-tuple elements, morphological set transformations can be performed on M by means of S. The two basic morphological transformations, namely dilation and erosion can be performed based on the *Hit or Miss principle*.[20] The dilation [Eq. (1)] and erosion [Eq. (2)] of M by S are defined as the set of all points m that the translated S_m intersects and contains in M. Ensuing are the mathematical and diagrammatic (Figs. 1 and 2) representations of these transformations.

Dilation: Let M and S be sub-images of Euclidean plane, IR^2. The dilation of an image, M, with

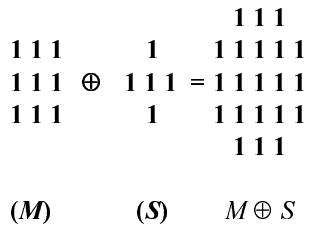

All translates of M by S are diagrammatically shown as follows

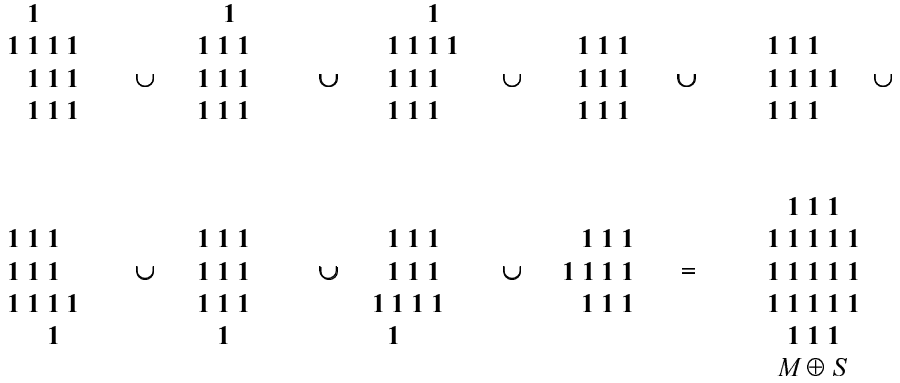

Fig. 1 Diagrammatic representation of morphological dilation process.

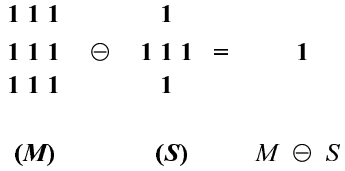

All translates of *M* by *S* are diagrammatically shown as follows

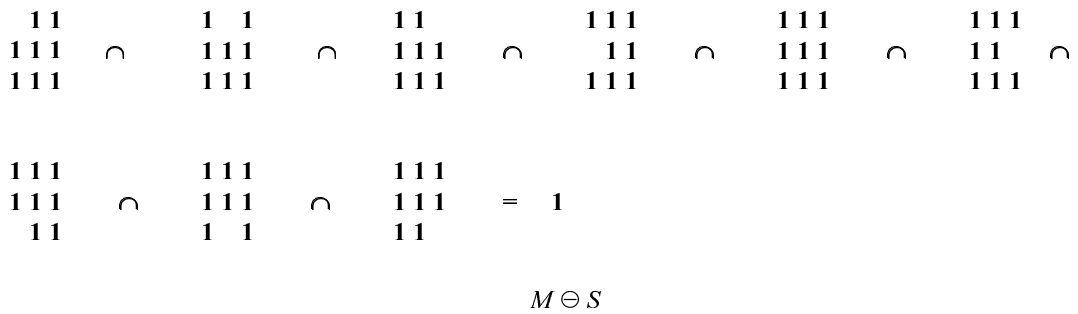

Fig. 2 Diagrammatic representation of morphological erosion process.

structuring element, S, is defined as

$$M \oplus S = \{m : S_m \cap M\} = \bigcup_{s \in S} M_s \,. \qquad (1)$$

Figure 1 shows the sequential steps involved in the process of dilation of M by means of a structuring element. A bounded S (Fig. 1), a circle in four-connectivity grid, that possesses a designed shape that is thought of a probe of M was used as a structuring element. All translates of M by S during dilation process are also digrammatically represented in Fig. 1.

Erosion: Let M and S be sub-images of Euclidean plane, IR^2. The erosion of an image, M, with

structuring element, S, is defined as

$$M \ominus S = \{m : S_m \subset M\} = \bigcup_{s \in S} M_s \,. \qquad (2)$$

Erosion of set M by structuring element S is diagrammatically shown along with all the translates in Fig. 2.

As structuring element $S = \check{\mathbf{S}}$, Minkowski's addition and subtraction are equivalent to morphological dilation and erosion, respectively. The considered structuring element $S = \check{\mathbf{S}}$ in the present study. Two consecutive erosions and dilations can be respectively represented as $(M \ominus S) \ominus S = M \ominus S_2$ and $(M \oplus S) \oplus S = M \oplus S_2$. The erosion followed by dilation is called *opening* transformation. How these basic morphological transformations are employed to extract channel networks [Eqs. (7) and (8)] from a simulated fractal basin are elucidated both mathematically and diagrammatically.

2.2 Horton's Laws of River Networks

In the geomorphological analysis of river networks, scaling properties are defined by Horton's laws,[21–23] and Strahler's[22] stream ordering yields the bifurcation stream number, and the stream length ratios. Horton's laws of channel network composition, stated in terms of Strahler's ordering technique, is considered here. A system of ordering that recognizes the existence of hierarchy among the separate segments is therefore assumed to represent the structure of channel networks. This postulates that source channels are of order 1, and when two channels of order i and j merge, a channel of order ω is formed, with

$$\omega = \max\{i,\, j,\, \mathrm{Int}[1 + (1/2)(i + j)]\} \qquad (3)$$

where function Int[ ] denotes the integer part. Following Eq. (3), when two channels of equal order join, a stream of the next order is formed, and when two streams of different orders join, the continuing channel retains the order of the higher-order channel. Horton's laws are described to appreciate their application in the *F-SCN* model. These empirical laws of stream numbers, and stream lengths[23] state that the bifurcation ratio R_B, and the stream length ratio R_L are constant for homogeneous river basins. Estimates of these ratios can be obtained from the slopes of the straight lines resulting from logarithmic plots of the transformed values of $N(\omega, \Omega)$, and $L(\omega, \Omega)$, versus order ω, for ω ranging from 1 to Ω.

Bifurcation ratio (R_B) is the ratio of number of stream segments of a given order $N(\omega - 1, \Omega)$ to the number of streams to the next highest order, $N(\omega, \Omega)$.

$$\frac{N(\omega - 1, \Omega)}{N(\omega, \Omega)} = R_B \quad \omega = 2, \ldots, \Omega \,. \qquad (4)$$

Stream length ratio (R_L) is the ratio of mean length of segments of order ω, $L(\omega, \Omega)$ and mean length of segments of the immediate lower order, $L(\omega - 1, \Omega)$.

$$\frac{L(\omega, \Omega)}{L(\omega - 1, \Omega)} = R_L \quad \omega = 2, \ldots, \Omega \qquad (5)$$

where $N(\omega, \Omega)$ is the number of streams of order ω in a basin of order $\Omega (N(\Omega, \Omega) = 1)$; $L(\omega, \Omega)$ is the average length of stream order ω; R_B and R_L are Horton's bifurcation and length ratios, respectively. These two standard morphometric quantities expressed in Eqs. (4) and (5) are directly used to compute the fractal dimension (D) of the river network[24] as follows:

$$D = \mathrm{Log}\, R_B / \mathrm{Log}\, R_L \,. \qquad (6)$$

3. FRACTAL-SKELETAL BASED CHANNEL NETWORK (*F-SCN*) MODEL

The river network pattern is determined due to boundary constraints. The river network paths can be defined as the union of all possible crenulation points that belong to successive erosion frontlines of the basin. From the cartographic point of view, crenulations are the protrusions that can be seen in a topographic contour as Λ- and V-shaped portions. These protrusions are the crenulations through which the river network flows. Hence, any basin outline needs to be simulated keeping this aspect in view. The basin outline should possess these crenulations. The number of crenulations increase with increasing resolution. However, it is a known fact that the area of the basin does not change with the change of scale. Hence, a typical generating mechanism that preserves the area as constant with increasing iterative process is employed to simulate the basin at different scales. Although the basin area does not change, the length of internal abstract structure, which is referred to as channel network in this paper, varies with succession of scale change.

To generate a model that conforms to the natural river basin, at least in statistical sense, it is essential to have the broad outline of the basin in the form of a polygon (i.e. an initiator), and the generating mechanism which transforms the initiator as a fractal basin. Generating mechanism needs to be designed by considering the following conditions.

(a) Area of the basin should be constant under succession of change in scale.
(b) The basin outline should possess increasing number of crenulations with increasing number of iterations.
(c) With iterative process to simulate basin outlines, the basin outlines should not self-intersect.
(d) The length of river network should increase with increasing iteration.

The generating mechanism plays an important role while transforming the initiator as a fractal basin. Homogeneous and heterogeneous channel network patterns result respectively by symmetric generator with non-random rule, and either symmetric or asymmetric generator with random rule. Also, the characteristics of the network depend on the overall shape of the initiator-basin. Asymmetric fractal basins arise due to asymmetric outline of the initiator, and due to generating mechanism as well as the adopted rule to transform the initiator as fractal basin. The accuracy in simulation of stream network depends on the generating mechanism, which includes the deterministic quantities like bifurcation ratio, stream length ratio and angle of divergence, the concept of skeletonization, and the rule (either random or non-random). This model has two sequential phases.

3.1 Fractal Basin Generation

To generate fractal basins with fractal dimensions ranging from 1 to 2 in two-dimensional space, one begins with two shapes: (1) broad outline of the basin as polygon, an initiator-basin, and (2) a generator. The latter is an oriented broken line made up of N equal sides of length r.[1] Each stage of the construction begins with a broken line and consists in replacing each straight interval with a copy of the generator, reduced and displaced to have the same end points as those of the interval being replaced. In all cases, $D = \mathrm{Log}\, N/\mathrm{Log}(1/r)$. Step 0 is to draw the segment of length (0, 1), which is one side length in the initiator-basin. Step 1, is to draw the kinked curves each made up of N intervals superposable upon the segment. Step 2, is to replace each of the N segments used in step 1 by a kinked curve obtained by reducing the curve of step 1 in the ratio $r(N) = 1/r$. One obtains all together N^2 segments of length $1/(r)^2$. Iterating this process adds further details. This process of generating fractal basin is based on the principle involved in the generation of Koch curves by considering the bounded initiator-basin. The boundary of the fractal basin possesses many crenulations referred to as *supremums* and *infemums* of which the connectivity network of the former is considered as flow path of the stream network. These crenulations in the outline of the fractal basin, and in the successive erosion frontlines determine the whole channel network pattern.

3.2 Channel Network Extraction

Channel network, a line thinned caricature that summarize the shape, size, orientation and connectivity of the basin can be extracted from the fractal basin. Components of such networks include traditional characteristics of shape in two-dimensional space. The channel network, $CH(M)$, of a fractal basin, (M), viewed as a subset of IR^2 (Euclidean space), can be defined mathematically as

$$CH_n(M) = (M \ominus S_n)\backslash\{[(M \ominus S_n) \ominus S] \oplus S\} \qquad n = 1, 2, \ldots, N \quad (7)$$

$$CH(M) = \bigcup_{n=0}^{N} CH_n(M) \quad (8)$$

where $CH_n(M)$ denotes the nth channel subset of fractal basin (M). In the above expression, subtracting from the eroded versions of M, their opening by S retains only the angular points, which are the channel points or subsets in this model. The union of all such possible channel points produces *F-SCN*. The structuring element (S) used in this channel network extraction from the simulated fractal basin is rhombus type. The diagrammatic representation of the steps involved in Eqs. (7) and (8) has been shown in Fig. 3.

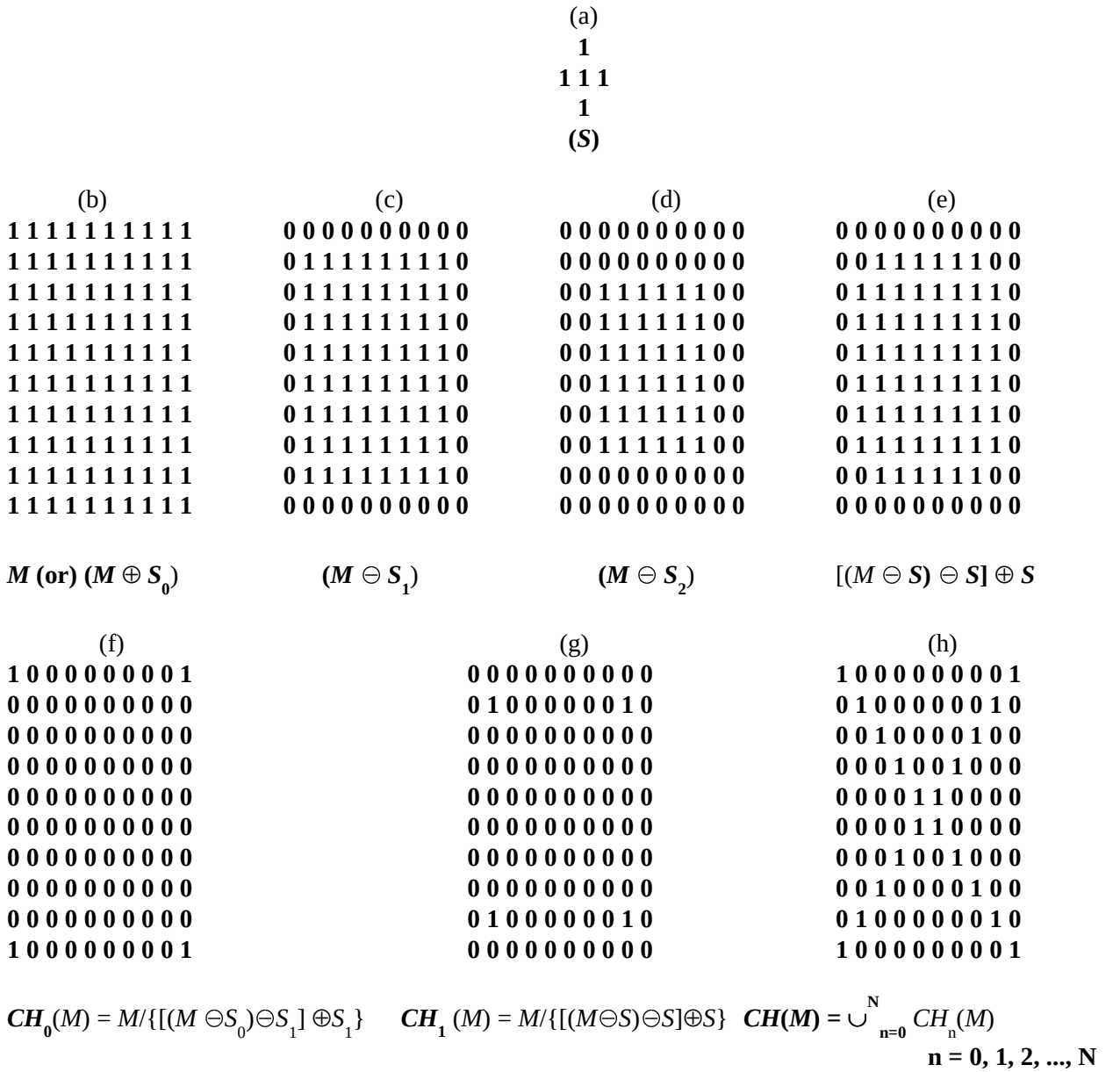

Fig. 3 **(a)** Structuring element, **(b)** hypothetical basin, **(c)** eroded basin, **(d)** erosion of eroded basin, **(e)** opening of eroded basin, **(f)** channel subsets of order zero, **(g)** channel subsets of first order, and **(h)** channel network of a hypothetical basin shown in **(b)**.

In other words, this algorithm is aimed to extract the set of all the centroids of the maximal disks that can be inscribed inside the basin, with a condition that the disk is maximal if it is not properly contained in any other disk totally included in the basin. Hence, a maximal disk must touch the boundary of the basin at least at two different points of the basin outline. The union of these centroids of the maximal disks inscribable in a fractal basin is *F-SCN*.

4. CASE STUDY, RESULTS AND CONCLUSIONS

The simulations have been carried out by considering a triangular initiator-basin (Fig. 4) with vertices at the bottom as outlet, and a generating mechanism shown in Fig. 5. Keeping the four conditions in view, a generating mechanism, which is akin to Koch generator, is defined (Fig. 5) to transform initiator-basin as a fractal basin. The

Fig. 4 A triangular initiator basin.

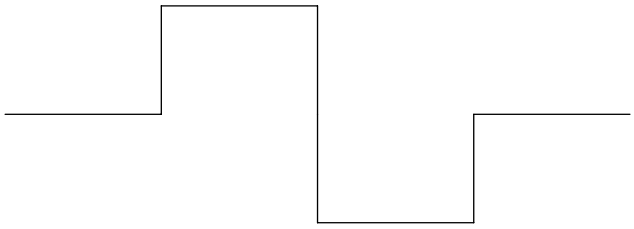

Fig. 5 A generating mechanism.

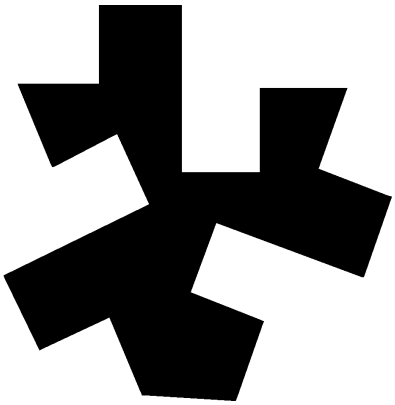

(a)

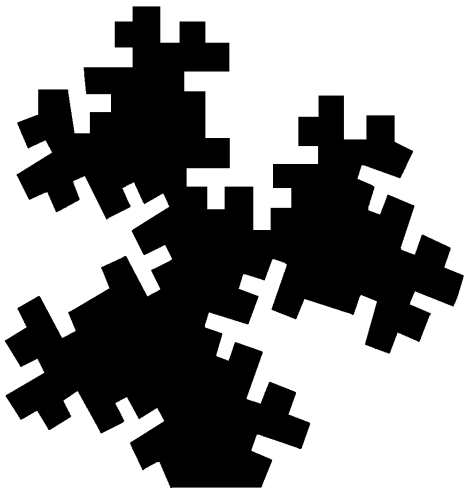

(b)

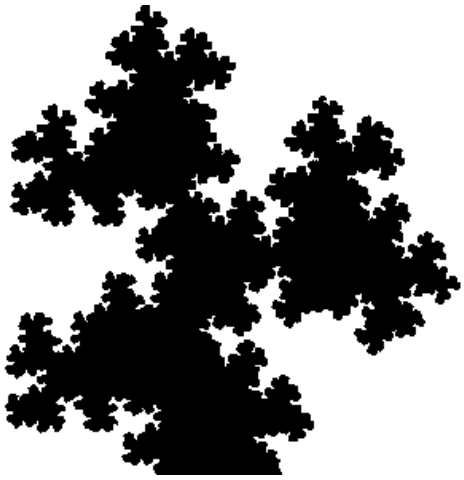

(c)

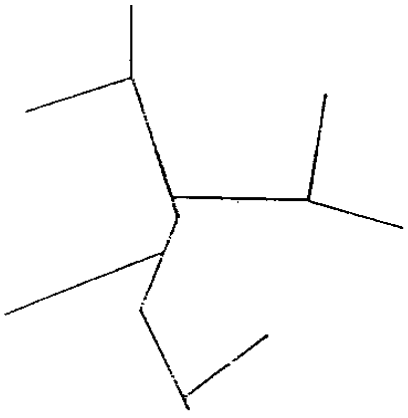

(d)

Fig. 6 **(a)**, **(b)** and **(c)** Fractal basins after respective iterations. **(d)**, **(e)** and **(f)** An evolutionary sequence of *F-SCNs* after respective iterations.

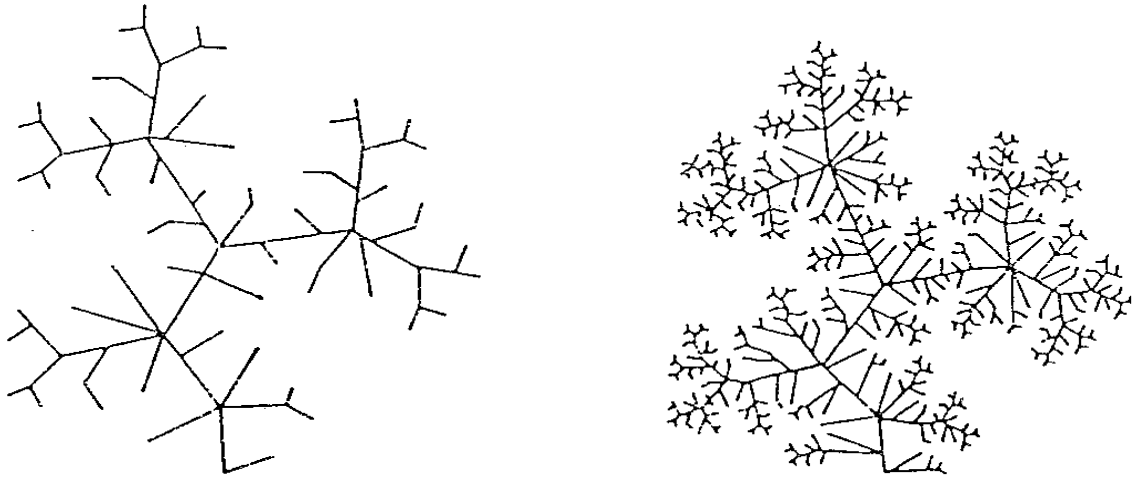

(e) (f)

Fig. 6 (*Continued*)

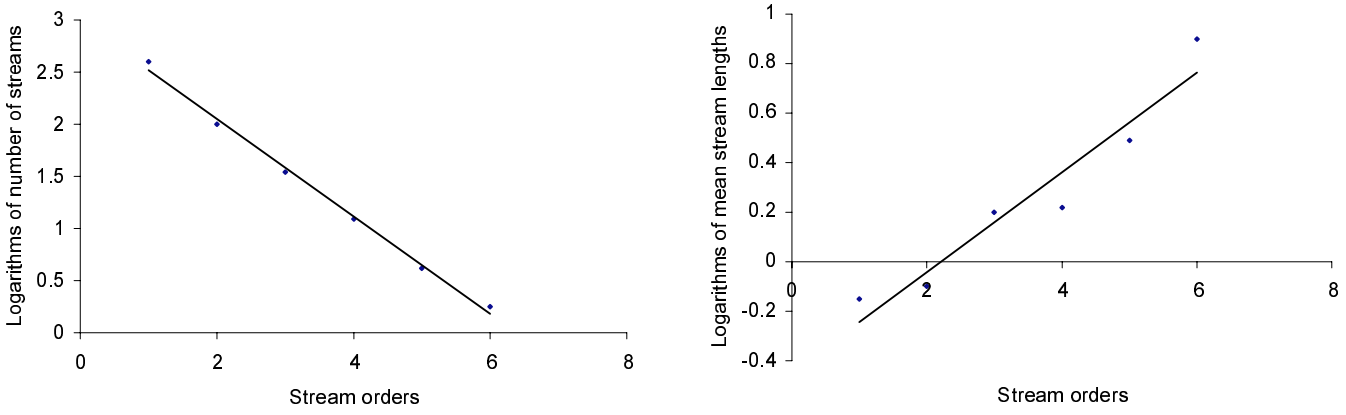

(a) (b)

Fig. 7 Statistical results of *F-SCNs* from triangular initiator-basin. **(a)** The log of the number of channel segments of a given order plotted against that order, and **(b)** the log of the average length of channel segments of a given order plotted against that order. Horton's laws state that a natural drainage basins will yield a linear relation on each graph.

simulated fractal basin outline, at different resolutions, possesses crenulations of various orders. To extract the morphological skeleton, which is referred to as channel networks, from the fractal basin by extracting all possible crenulations from all possible erosion frontlines of the fractal basin, a set of simple morphology-based equations described in Sec. 2.1, have been applied to generate *F-SCNs* from the fractal basins [Figs. 6(a)–(c)] thus simulated. An evolutionary sequence of *F-SCNs* is given in Figs. 6(d)–(f). In this model, the study of boundary constrained growth of drainage is given emphasis. It is observed that the competition among the sub-networks is due to the dominance of a few major stream systems. Furthermore, the organization of the channel networks appears more expeditiously relative to the total number of possible iterations. By the third iteration, the maximum order of the networks ($\Omega = 7$) has been established, and under subsequent iterations the lower order channels occupy more space. As opined by Rodriguez-Iturbe et al.[15] in the context of developing a framework of river basin morphology based on *OCNs* and in the present *F-SCN* model, the boundary of

the basin clearly forces the development of channel networks. Figure 6(f) bears a striking qualitative resemblance to the natural channel networks. Similar to the patterns of headward erosion seen in nature, *F-SCN* growth produces headward evolving channel patterns with increasing number of iterations. The dependencies of number and mean length of channels on order number for *F-SCNs* after third iteration are plotted. A linear relationship [Figs. 7(a) and (b)] is observed in both the plots, which indicates that the *F-SCNs* follow Horton's laws.

The variation of the channel density with increasing number of iterations also indicates that the *F-SCN* is Hortonian. Using Eqs. (4) and (5), the bifurcation ratio (R_B) and the stream length ratio (R_L) are computed as 2.74 and 1.78, respectively. The computed value of the fractal dimension from Eq. (6) is 1.76 which is near to the observed value 1.8.

The *F-SCN* model produces channel networks that bear a strong resemblance to real networks, evolve headward through time, and yields a fractal dimension of 1.76 that is less than the fractal dimension value of 2 for space-filling channel networks. As the considered initiator-basin is of triangular type, and the generating mechanism maintains the constancy of the area during the succession of changes, and the channel network pattern that arises is of the dendritic type. The mechanism involved is analogous to the mechanism operating in a natural drainage system. More natural channel networks may be simulated by considering either asymmetric generating mechanism with a random rule or irregular initiator-basin, or both, and the varied characteristic information of the structuring element (S). The characteristic information of structuring element plays a vital role in the skeletonization process that extracts the channel networks from the simulated fractal basin at a specific scale. The potential applications of fractals to develop algorithms for modeling drainage morphogenesis can be studied. The utility of this approach is that one can explore developmental and morphogenic hypothesis with varying initiator, generator specifications, structuring element characteristics, skeletonization process and the involved rule to transform the initiator by a generator as a fractal basin.

ACKNOWLEDGMENT

The authors are grateful to an anonymous referee for his comments and suggestions.

REFERENCES

1. B. B. Mandelbrot, *Fractal Geometry of Nature* (Freeman, New York, 1982), p. 468.
2. E. E. H. Culling, *J. Geol.* **68**, 336–344 (1960).
3. L. B. Leopold and W. B. Langbein, *US Geol., Surv. Prof. Pap.* **A500** (1982).
4. H. Shenck, *J. Geophys. Res.* **68**, 5739–5745 (1963).
5. R. L. Shreve, *J. Geol.* **77**, 397–414 (1967).
6. A. E. Sheideggar, *Bull. Int. Assoc. Sci. Hydrol.* **12**(1), 15–20 (1967).
7. H. Kondoh and M. Matsushita, *J. Phys. Soc. Japan* **55**, 3289–3292 (1986).
8. A. D. Howard, *Water Resour. Res.* **26**(9), 2107–2117 (1990).
9. C. P. Stark, *Nature* **352**, 423–425 (1991).
10. P. Meakin, J. Feder and T. Jossang, *Physica* (Amsterdam) **A176**, 409–429 (1991).
11. G. Huber, *Physica* **A170**(3), 463–470 (1991).
12. G. Wilgoose, R. L. Bras and I. Rodriguez-Iturbe, *Water Resour. Res.* **27**, 1671–1684 (1991).
13. C. G. Chase, *Geomorphology* **5**, 39–57 (1992).
14. S. Kramer and M. Marder, *Phys. Rev. Lett.* **68**, 205–208 (1992).
15. I. Rodriguez-Iturbe, A. Rinaldo, R. Rigon, R. L. Bras and E. Ijjasz-Vasquez, *Water Resour. Res.* **28**(4), 1095–1103 (1992).
16. J. Masek and D. L. Turcotte, *Ear. Plan. Sci. Lett.* **119**, 379–386 (1993).
17. A. Rinaldo, I. Rodrigues-Iturbe, R. L. Bras and E. Ijjasz-Vasquez, *Phys. Rev. Lett.* **70**, 822–826 (1993).
18. B. S. D. Sagar, *Chaos, Solitons and Fractals* **7**(11), 1871–1879 (1996).
19. B. S. D. Sagar, C. Omoregie and B. S. P. Rao, *Discr. Dyn. Nat. Soc.* **2**(2), 77–92 (1998).
20. J. Serra, *Image Analysis and Mathematical Morphology* (Academic Press, New York, 1982), p. 610.
21. R. E. Horton, *Bull. Geophys. Soc. Am.* **56**, 275–370 (1945).
22. A. N. Strahler, in *Handbook of Applied Hydrology*, ed. V. T. Chow (McGraw-Hill, New York, 1964), pp. 4–39 to 4–76.
23. J. S. Smart, *Adv. Hydrosci.* **8**, 305–346 (1972).
24. P. La Barbera and R. Rosso, *Eos. Trans. AGU* **68**(44), 1276 (1987).